Efficient intensity-gradient cooling of atoms in a weak standing-wave hollow-beam trap

Zhengling Wang[1,2] and Jianping Yin[1,*]

[1]*Key Laboratory for Optical and Magnetic Resonance Spectroscopy of Ministry of Education, Department of Physics, East China Normal University, Shanghai 200062, People's Republic of China*

[2]*Department of Physics, Jiangsu University, Zhenjiang 212013, People's Republic of China*

(Received 3 April 2006; published 21 July 2006)

We propose a trap scheme for cold alkali-metal atoms with an efficient intensity-gradient induced Sisyphus cooling in a weak standing-wave hollow-beam gravito-optical trap, which is composed of the interference of two well collimated, counterpropagating doughnut hollow beams with an intensity difference and a plug beam. We calculate the intensity distribution of the weak standing-wave hollow-beam field and its intensity gradient one, and find that such an optical dipole trap with an extremely high intensity gradient is desirable to realize an efficient intensity-gradient cooling for alkali-metal atoms in the trap. We also calculate the optical potentials, instantaneous dipole forces and spontaneous emission rates for a three-level dressed atom and study the dynamic process of intensity-gradient cooling of ^{87}Rb atoms in the weak standing-wave hollow-beam trap by Monte Carlo simulations. Our study shows that the minimum optical potential at each node in our dipole trap is high enough to trap almost all cold atoms with a temperature of 120 μK released from a standard magneto-optical trap, and an ultracold ^{87}Rb atomic sample with a temperature of $\sim$0.73 μK can be obtained in the trap. Starting from this stage, an all-optical Bose-Einstein condensation (BEC) could be realized by using the optical-potential evaporative cooling.

DOI: 10.1103/PhysRevA.74.013408 PACS number(s): 32.80.Pj, 32.80.Lg, 42.50.Vk

I. INTRODUCTION

It is well known that sub-Doppler laser cooling mechanisms of neutral atoms can be classified as polarization-gradient cooling (PGC) [1] and intensity-gradient one [2]. So called "intensity-gradient cooling (IGC)," that is an intensity-gradient induced Sisyphus cooling of neutral atoms trapped in a blue-detuned inhomogeneous light field, such as a standing-wave light field, or an evanescent-wave light field, or a dark hollow-beam field. The cooling mechanism of the IGC can be briefly described as follows: In the dressed-state picture as shown in Fig. 1, when an atom in the lower dressed state $|1,n\rangle$ entering a blue-detuned inhomogeneous (i.e., intensity gradient) light field can make a spontaneous transition to the less repulsive upper dressed state $|2,n-1\rangle$ by scattering a photon. Soon after the inelastic reflection of the atom from the blue-detuned light field, the atom is pumped back to the original dressed state $|1,n-1\rangle$ by the repumping beam. Then, a closed and repeatable Sisyphus cooling cycle is formed, and the loss of the atomic kinetic energy is proportional to the difference (U_1-U_2) between the light-shift potentials of two dressed states. So this Sisyphus cooling resulting from the intensity gradient of the inhomogeneous light field is usually called intensity gradient cooling [2], and such an IGC was demonstrated both theoretically and experimentally in a blue-detuned standing-wave light [3,4] and a blue-detuned evanescent-wave light [5–7], or a blue-detuned hollow beam [8–12].

A gravito-optical trap (GOT) for cold atoms with evanescent-wave induced Sisyphus cooling was proposed and demonstrated experimentally, and an ultracold Rb (or Cs) atomic sample with a temperature of $\sim$10 μK (or $\sim$3 μK) was obtained [5–7]. Although the intensity gradient of the evanescent-wave light is very high, its optical potential will be rapidly weakened by van der Waals attractive potential near the interface of a mirror. So the atoms will be stuck to the surface of the mirror and then lost from the GOT if the kinetic energies of some atoms are larger than the optical potential. In addition, it is not easy to manipulate and control the motion of cold atoms by using evanescent-wave light field. To overcome these disadvantages, a new GOT using a blue-detuned dark hollow beam (DHB) was proposed to trap cold atoms, even to cool them by using the DHB-induced IGC [8–12]. However, since the intensity gradient inside a doughnut-hollow beam or other DHBs is far smaller than one in the evanescent-wave light field, the DHB-

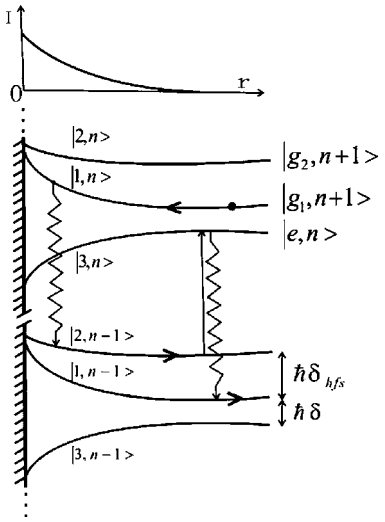

FIG. 1. Dressed-states picture of the three-level atom and basic principle of intensity-gradient induced Sisyphus cooling of atoms in a blue-detuned, inhomogeneous light field.

*Corresponding author. Email address: jpyin@phy.ecnu.edu.cn

induced Sisyphus cooling effect is much less than the evanescent-wave induced one, which was verified both theoretically [11] and experimentally [13], also by our simulated results [see Fig. 9(a)]. So it would be interesting and worthwhile to find some new hollow-beam traps so as to realize an efficiently DHB-induced IGC, even to realize an all-optical atomic BEC in a blue-detuned hollow-beam trap.

In 2001, Yin *et al.* proposed a GOT using a blue-detuned, pyramidal-hollow beam (PHB) and investigated the PHB-induced IGC of alkali-metal atoms by using Monte Carlo simulations [14], and found that an ultracold ^{133}Cs atomic sample with a temperature of $\sim 2\ \mu$K can be obtained in the PHB GOT. To further improve the DHB-induced IGC, in this paper, we propose a unique GOT scheme to trap and cool neutral atoms by using a weak standing-wave hollow-beam GOT and its efficient IGC, and study the dynamic process of the IGC of ^{87}Rb atoms in our proposed GOT by Monte Carlo simulations. In Sec. II, we present a GOT scheme and analyze the intensity distribution of our weak standing-wave hollow-beam field and its intensity gradient profile. In Sec. III, to perform a Monte Carlo study under the case of strong light-atom interaction, we use the dressed atomic approach to derive more exact analytic expressions on the optical potentials, instantaneous dipole forces and spontaneous emission rates for a three-level dressed-atom in a light field. In Sec. IV, we study the dynamic process of the IGC of ^{87}Rb atoms in our GOT by Monte Carlo simulations, and obtain some new and interesting results. The main results and conclusions are included in the final section.

II. SCHEME OF WEAK STANDING-WAVE HOLLOW BEAM GOT

Our unique trap scheme with an efficient IGC of atoms is shown in Fig. 2. A blue detuned, linearly polarized, well-collimated doughnut-hollow beam is propagated downwards, and reflected upwards by a mirror M, and then a standing-wave hollow-beam field will be formed. To avoid cold atoms escape from a series of nodes of the standing-wave hollow-beam field, an intensity modulator (IM) in the front of the mirror is used to adjust the intensity of the reflected beam from zero to a maximum one, which will provide a minimum optical potential at each node where cold atoms cannot be lost from each node. Then a weak standing-wave hollow-beam gravito-optical trap (GOT) for cold atoms will be formed above the blue-detuned plug beam. Since the standing-wave hollow-beam field has a high intensity gradient, our GOT cannot only be used to trap cold atoms, but also to efficiently cool the trapped atoms combined with a weak, near-resonant repumping beam (WRB) propagating downwards.

The electric field distributions of two linearly-polarized doughnut-hollow beams that propagate in the opposite direction can be described by two standard TEM_{01}^{*} doughnut beams, and in the polar coordinates given respectively by

$$E_1(r,\phi,z) = E_{01}\exp(i\phi)\exp[i(\omega t + kz)], \tag{1a}$$

$$E_2(r,\phi,z) = E_{02}\exp(i\phi)\exp[i(\omega t - kz)], \tag{1b}$$

where

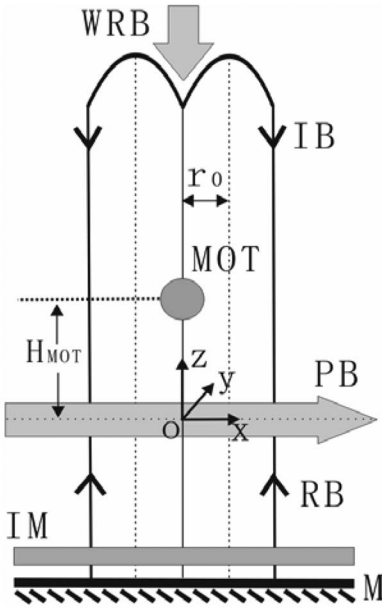

FIG. 2. Scheme of the gravito-optical trap for cold atoms using a weak standing-wave hollow-beam field and a gravity field. M, MOT, IB, RB, PB, IM, and WRB stand for mirror, magneto-optical trap, input beam, reflected beam, plug beam, intensity modulator, and weak repumping beam, respectively.

$$E_{01} = \sqrt{\frac{P_1}{\pi}}\frac{2r}{w^2}\exp\left(-\frac{r^2}{w^2}\right), \tag{2a}$$

$$E_{02} = \sqrt{\frac{P_2}{\pi}}\frac{2r}{w^2}\exp\left(-\frac{r^2}{w^2}\right), \tag{2b}$$

where w is the waist of the well-collimated doughnut-hollow beam and can be regarded as a constant, P_1 and P_2 are the powers of input hollow beam and reflected one, respectively. For the sake of convenience, we define a beam parameter η (we called it "standing-wave parameter") to describe the intensity ratio of the incident hollow beam to the reflected one, that is, $\eta = P_2/P_1$, which can be adjusted from 0 to 1.0 by using the intensity modulator IM. It is clear that $\eta = 0$ and $\eta = 1$ represent a single traveling-wave hollow-beam light field and a standard standing-wave one, respectively, while the case of $0 < \eta < 1$ stands for a weak standing-wave hollow-beam field. The intensity distribution of the standing-wave hollow-beam field is given by

$$I = E_{01}^2 + E_{02}^2 + 2E_{01}E_{02}\cos(2kz). \tag{3}$$

From Eq. (3), we can see that the intensity distribution in the z direction is periodic with a spatial period of $\lambda/2$. When $\eta = 1$, there are a series of zero-intensity rings at $z = (2n+1)\lambda/4$ (i.e., at each node) in the standing-wave hollow-beam field, here n is integer. In or near these rings, cold atoms released from a standard magneto-optical trap (MOT) will be escaped from the standing-wave hollow-beam GOT. So we should choose the standing-wave parameter η to make the optical potential at $z = (2n+1)\lambda/4$ far larger than the root-mean-square (rms) kinetic energy of cold atomic sample so

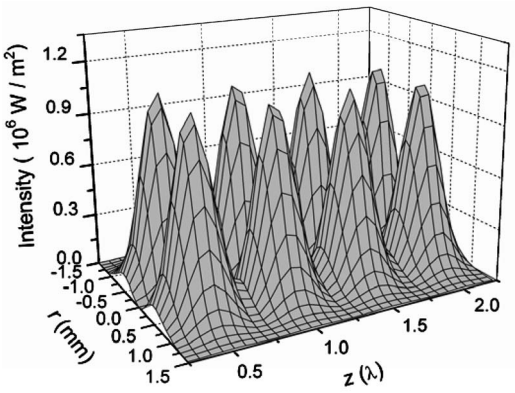

FIG. 3. The intensity distribution of the weak standing-wave hollow-beam light field for $r_0=0.5$ mm, $P_1=1000$ mW, and $\eta=0.28$.

as to let nearly all cold atoms stay in the GOT. When the beam radius of the DHB is $r_0=0.5$ mm, and taking $P_1=1000$ mW and $\eta=0.28$, we calculate the intensity distribution of the weak standing-wave hollow-beam field, and the result is shown in Fig. 3. We can find from Fig. 3 that the maximum intensity is 1.1×10^6 W/m^2 at $z=n\lambda/2$ as $r=r_0$ and the minimum intensity is 1.0×10^5 W/m^2 at $z=(2n+1)\lambda/4$ as $r=r_0$, the corresponding optical potential will be greater than atomic rms kinetic energy (see below).

The intensity gradient distribution of our standing-wave hollow-beam field is given by

$$\nabla I=\frac{\partial I}{\partial r}\hat{\mathbf{r}}+\frac{\partial I}{\partial z}\hat{\mathbf{z}}, \tag{4}$$

where the radial and axial intensity gradients are given respectively by

$$\frac{\partial I}{\partial r}=[2E_{01}^2+2E_{02}^2+4E_{01}E_{02}\cos(2kz)]\left[\frac{1}{r}-\frac{2r}{w^2}\right], \tag{5a}$$

$$\frac{\partial I}{\partial z}=-4kE_{01}E_{02}\sin(2kz). \tag{5b}$$

It is clear from Eqs. (3) and (4) that the axial intensity gradient inside the traveling-wave hollow beam (i.e., when $\eta=0$) in the z direction will be zero. From Eq. (5), we calculate the dependence of the radial and axial intensity gradients on the radial position r (and on the propagation distance z) as $r_0=0.5$ mm, $P_1=1000$ mW, and $\eta=0.28$, and find that the maximum radial intensity gradient inside the weak standing-wave hollow beam is about two times that inside the traveling-wave hollow beam (its maximum intensity gradient is about 1.9×10^9 W/m^3). We also find that the maximum axial intensity gradient can be reached 8×10^{12} W/m^3, which is about 8 times that of the evanescent-wave surface trap (9.7×10^{11} W/m^3) in Ref. [7]. So the IGC of atoms in our weak standing-wave hollow-beam GOT will be more efficient than that of the evanescent-wave surface trap [7].

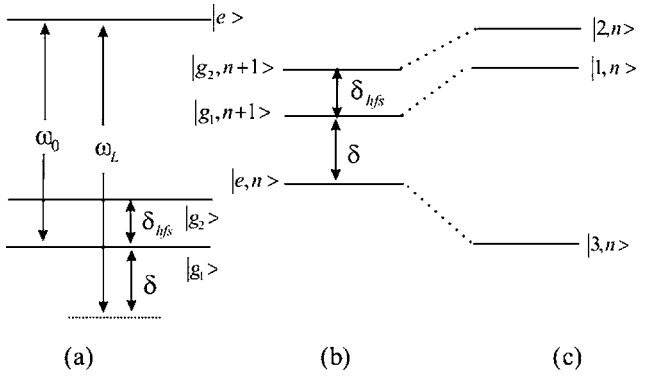

FIG. 4. Atomic energy-level diagram: (a) Λ-configuration three-level atom diagram; (b) States of the combination of atom-laser mode system without the coupling, which are bunched into three-dimension manifold E_n; (c) Atom-laser mode coupling produces the dressed atom states.

III. QUASIANALYTIC SOLUTIONS OF A THREE-LEVEL DRESSED-ATOM SYSTEM

A. Eigenenergies and optical potentials

We consider a Λ-configuration three-level atom with one excited state $|e\rangle$ and two hyperfine ground states $|g_1\rangle$ and $|g_2\rangle$, which is interacted with an intense laser field with a frequency of $\omega_L/2\pi$ and a detuning of $\delta/2\pi$ from the atomic resonant frequency $\omega_0/2\pi$ between the lower hyperfine ground state $|g_1\rangle$ and the excited state $|e\rangle$, as shown in Fig. 4(a). If the coupling between the laser mode and the atom is not considered, the eigenstates of the dressed Hamiltonian are bunched in the well-separated three-dimension manifolds $E_1,\ldots,E_{n-1},E_n,\ldots$, which are separated by the energy of $\hbar\omega_L$, here n is integer. Each E_n manifold is composed of three states $|g_1,n+1\rangle$, $|g_2,n+1\rangle$, and $|e,n\rangle$ (atom in the internal states $|g_1\rangle$, $|g_2\rangle$, or $|e\rangle$ with $n+1$, $n+1$, or n laser photons), as shown in Fig. 4(b).

We assume that the detuning $|\delta|$ between ω_L and ω_0 is much lower than ω_L or ω_0, so we can safely neglect the coupling between different three-dimension manifolds. Moreover, the diagram of the dressed Hamiltonian is periodic, and in which there are many (or infinity) invariable three-dimension subspaces. Corresponding to three-dimension manifold of E_n, the equation of eigenstates (considering atom-laser mode coupling) in the dressed-state picture can be written by

$$\hbar\begin{pmatrix}(n+1)\omega_L+\delta_{hfs} & 0 & G_2\sqrt{n+1}\\ 0 & (n+1)\omega_L & G_1\sqrt{n+1}\\ G_2\sqrt{n+1} & G_1\sqrt{n+1} & n\omega_L+\omega_0\end{pmatrix}\begin{pmatrix}A_i\\B_i\\C_i\end{pmatrix}=E_{Dri}\begin{pmatrix}A_i\\B_i\\C_i\end{pmatrix}, \tag{6}$$

where $\delta_{hfs}/2\pi$ is the level splitting between two hyperfine ground states, and G_1 (G_2) is a real coupling parameter corresponding to Rabi frequency Ω_1 (Ω_2) between $|g_1,n+1\rangle(|g_2,n+1\rangle)$ and $|e,n\rangle$ by $\Omega_1=2G_1\sqrt{n+1}$ and Ω_2

$=2G_2\sqrt{n+1}$. In Eq. (6), A_i, B_i, and C_i are the probability amplitudes respectively in $|g_2,n+1\rangle$, $|g_1,n+1\rangle$, and $|e,n\rangle$ corresponding to the dressed eigenstate $|i,n\rangle$ in the dressed atom picture, as shown in Fig. 4(c), here $i=1,2,3$.

Since the exact eigenenergies (see Appendix A) from Eq. (6) are too complex to give clear analytic relationships between the eigenenergies (or optical potentials) of three dressed eigenstates and the parameters $(\delta,\delta_{hfs},\Omega_1,\Omega_2)$ of atom-light interaction system, we cannot obtain analytic or quasianalytic solutions of the optical potentials, instantaneous dipole forces and spontaneous emission rates. For this reason, we substitute a trial solution $E^t_{Dr1}=(n+1)\hbar\omega_L-\hbar\delta/2\pm\hbar(\delta^2+\Omega_1^2)^{1/2}/2$ into Eq. (6), and then derive two other solutions E^t_{Dr2} and E^t_{Dr3}. Here the trial solution E^t_{Dr1} is the eigenenergy of the dressed eigenstate $|1,n\rangle$ coming from the two-level atom model [9,15,16], and E^t_{Dr2}, E^t_{Dr3} correspond to dressed eigenstates $|2,n\rangle$ and $|3,n\rangle$, respectively. To obtain a general (for any detuning) and more exact (with a permissible error) quasianalytic relationships between the eigenenergies and the parameters $(\delta,\delta_{hfs},\Omega_1,\Omega_2)$, by further substituting E^t_{Dr2} (which is one of the solutions in Ref. [17]) into Eq. (6), and adjusting the corresponding coefficients in front of (δ,Ω_1') and as well as considering the conservation of energy, we derive two other eigenenergies, by which we can obtain three more exact expressions of the eigenenergies corresponding to the dressed eigenstates $|1,n\rangle$, $|2,n\rangle$, $|3,n\rangle$ as follows:

$$E_{Dr1}=(n+1)\hbar\omega_L-\frac{\hbar\Delta}{2}\pm\frac{\hbar\sqrt{\Delta^2+\Omega_1^2}}{2}, \tag{7a}$$

$$E_{Dr2}=(n+1)\hbar\omega_L-\frac{\hbar}{2}(\Delta-\delta_{hfs})+\mathrm{sgn}\,\frac{\hbar\sqrt{(\Delta+\delta_{hfs})^2+\Omega_2^2}}{2}, \tag{7b}$$

$$E_{Dr3}=(n+1)\hbar\omega_L+\hbar\Delta-\hbar\delta+\frac{\hbar\delta_{hfs}}{2}\mp\frac{\hbar\sqrt{\Delta^2+\Omega_1^2}}{2}-\mathrm{sgn}\,\frac{\hbar\sqrt{(\Delta+\delta_{hfs})^2+\Omega_2^2}}{2}, \tag{7c}$$

where

$$\Delta\equiv\pm\frac{\Omega_1'}{32}+\frac{31\delta}{32} \tag{7d}$$

is defined as a generalized laser detuning, and "+" and "−" in "$\pm$" or "−" and "+" in "$\mp$" represent the case of $\delta>0$ and $\delta<0$, respectively, sgn is 1 when $\delta>-\delta_{hfs}$, and −1 when $\delta<-\delta_{hfs}$, which have the same meaning in the following equations. If we suppose that the laser field is initially in a coherent state with a Poisson distribution for n, and its width Δn is very small compared with the average photon number $\bar{n}$ and much larger than 1, we can neglect the dependence of Ω_1 and Ω_2 on the photon number n. In Eq. (7), $\Omega_1'=\sqrt{\delta^2+\Omega_1^2}$, and for the alkali-metal atom, Ω_j may be expressed by $\Omega_j=\sqrt{I/2I_{sat}}\Gamma f_j^{1/2}=\Omega f_j^{1/2}$, and I is the laser intensity, I_{sat} is the saturation intensity of the atom, $f_j=2/3$ is the relative transition strength from $|e\rangle$ to $|g_j\rangle$, $j=1,2$, $\Omega=\sqrt{I/2I_{sat}}\Gamma$, Γ is the spontaneous emission rate of the excited state $\langle e|$. Taking the atom of ^{87}Rb as an example, we compared E_{Dri} in Eq. (7) with the exact solutions from Eq. (6), here $i=1,2,3$. For a ^{87}Rb atom, $\delta_{hfs}/2\pi=6.835$ GHz, $I_{sat}=16$ W/m^2, and $\Gamma/2\pi=6.0$ MHz, we find from Appendix B that the maximum relative error between expressions $E_{Dri}-(n+1)\hbar\omega_L$ in Eq. (7) and the exact expressions [see Eqs. (A2) and (A3)] is about 3.0% as $I=2.5\times10^6$ W/m^2 for arbitrary detuning $\delta/2\pi$. This shows that Eq. (7) can be indeed regarded as a general and more exact solution of Eq. (6) and safely used to calculate the eigenenergies E_{Dri} and their optical potentials and eigenstates and so on for arbitrary detuning and $I\leqslant2.5\times10^6$ W/m^2.

From Eq. (7), we can obtain three general expressions of optical potentials corresponding to eigenenergies E_{Dr1}, E_{Dr2}, and E_{Dr3} in the dressed atomic system

$$U_1=-\frac{\hbar\Delta}{2}\pm\frac{\hbar\sqrt{\Delta^2+\Omega_1^2}}{2}, \tag{8a}$$

$$U_2=-\frac{\hbar}{2}(\Delta+\delta_{hfs})+\mathrm{sgn}\,\frac{\hbar\sqrt{(\Delta+\delta_{hfs})^2+\Omega_2^2}}{2}, \tag{8b}$$

$$U_3=\hbar\Delta+\frac{\hbar\delta_{hfs}}{2}\mp\frac{\hbar\sqrt{\Delta^2+\Omega_1^2}}{2}-\mathrm{sgn}\,\frac{\hbar\sqrt{(\Delta+\delta_{hfs})^2+\Omega_2^2}}{2}. \tag{8c}$$

Under the approximation of a small saturation parameter (that is, $\delta\gg\Omega\gg\Gamma$), we have $\Omega_1'=\sqrt{\Omega_1^2+\delta^2}\approx\delta$ and obtain $\Delta\approx\delta$ from Eq. (7d). Then substituting $\Delta\approx\delta$ into Eq. (8), we can derive the approximation expressions of optical potentials (U_1',U_2',U_3') corresponding to three dressed states $|1,n\rangle$, $|2,n\rangle$, and $|3,n\rangle$, and we find that they are the same as the expressions in Refs. [9,15,16], and can be further reduced to the results in Refs. [6–8,10]. The approximation expression of optical potential U_1' can be given by $U_1'=-\hbar\delta/2+\hbar\sqrt{\delta^2+\Omega_1^2}/2$. We compare U_1' with our U_1, and find that when $\delta/2\pi=1.0$ GHz, U_1' can only be used as $I<9.0\times10^3$ W/m^2 within the same ±3% error, which is far lower than our result ($I\leqslant2.5\times10^6$ W/m^2). In our GOT, if taking $r_0=0.5$ mm, $P_1=1000$ mW, $\eta=0.28$, the maximum intensity can be reached 1.1×10^6 W/m^2, so we cannot use expressions U_1', U_2', and U_3' to calculate optical potentials, but can use our Eq. (8) to calculate them. From Eq. (8), we calculate the distribution of the optical potential U_1 for a ^{87}Rb atom in our trap for $r_0=0.5$ mm, $P_1=1000$ mW, $\eta=0.28$, and $\delta/2\pi=1$ GHz, the result is shown in Fig. 5(a). We know from Fig. 5(a) that the maximum optical potentials along the z direction appear at $z=n\lambda/2$ (i.e., at each antinode), and the minimum optical potentials appear at $z=(2n+1)\lambda/4$ (i.e., at each node), here n is the integer. The optical potential U_2 is smaller than that of U_1 for the same parameters and the distribution of U_2 is similar to one of U_1.

To trap all atoms from a standard MOT, the minimum optical potential U_2 at $r=r_0$ should be larger than the rms kinetic energy of cold atomic sample. From Eq. (8), we calculate the dependence of optical potentials at $z=(2n+1)\lambda/4$

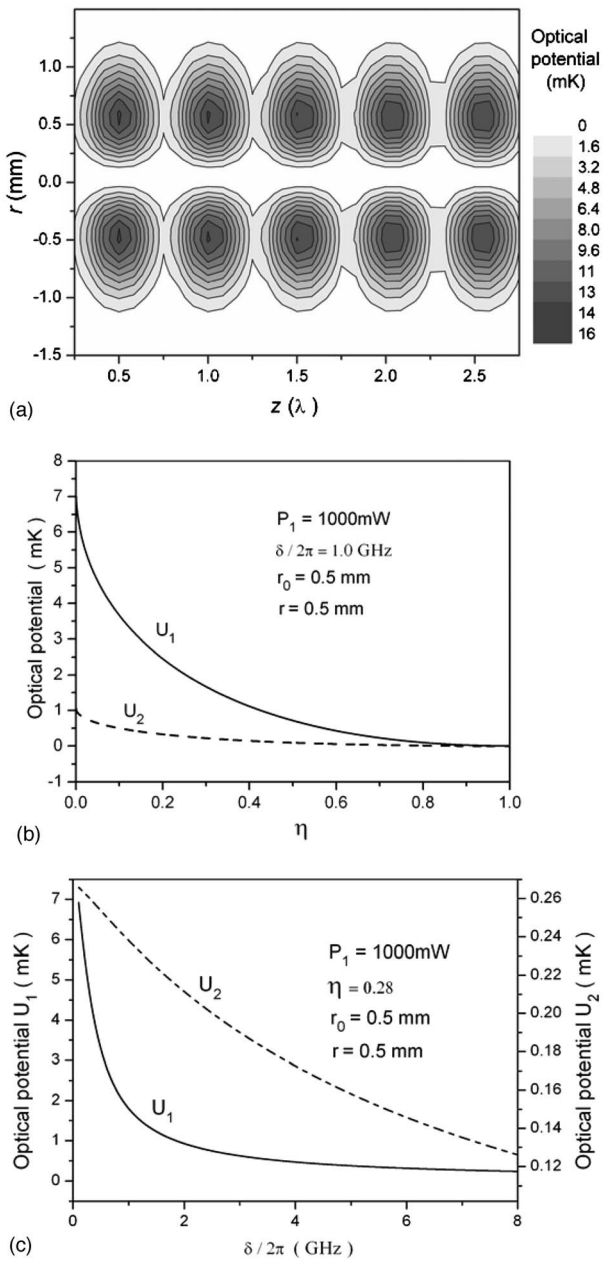

FIG. 5. The distribution of the optical potentials of an ^{87}Rb atom in the weak standing-wave hollow-beam light field. (a): The contour of the optical potential U_1 for $r_0=0.5$ mm, $P_1=1000$ mW, $\eta=0.28$, and $\delta/2\pi=1$ GHz; (b) Optical potentials at $z=(2n+1)\lambda/4$ versus η for $r=r_0=0.5$ mm, $P_1=1000$ mW, and $\delta/2\pi=1$ GHz; (c) Optical potentials at $z=(2n+1)\lambda/4$ versus $\delta/2\pi$ for $r=r_0=0.5$ mm, $P_1=1000$ mW, and $\eta=0.28$.

for a ^{87}Rb atom in our trap on the beam parameter η as $r=r_0=0.5$ mm, $P_1=1000$ mW, and $\delta/2\pi=1$ GHz, and the results are shown in Fig. 5(b). We find from Fig. 5(b) that the optical potential U_2 will be larger than 240 μK as $\eta\leqslant 0.28$, which is high enough to effectively capture almost all cold ^{87}Rb atoms from the MOT with a temperature of $\sim$120 μK. At $z=(2n+1)\lambda/4$, the dependence of the optical potentials on the detuning $\delta/2\pi$ is also calculated from Eq. (8) as $r=r_0=0.5$ mm, $P_1=1000$ mW, and $\eta=0.28$, and the results

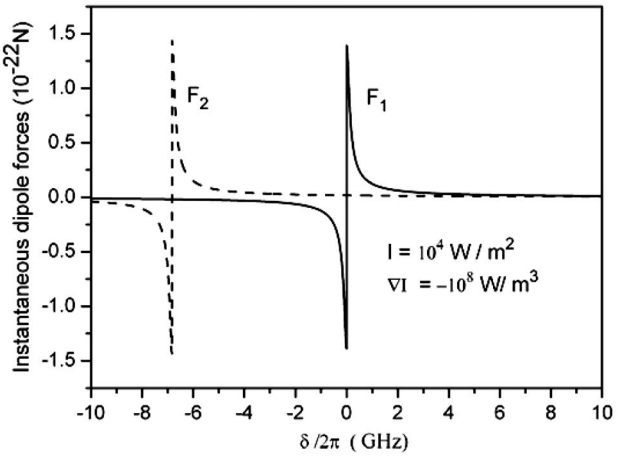

FIG. 6. Dependences of the instantaneous dipole force on the laser detuning $\delta/2\pi$ for $I=10^4$ W/m^2 and $\nabla I=-10^8$ mW/cm^3.

are shown in Fig. 5(c). We know from Fig. 5(c) that the optical potential U_2 will be larger than 120 μK, which is high enough to effectively capture most of cold atoms from the MOT as $\delta/2\pi<8$ GHz.

B. The instantaneous dipole force

An atom in an inhomogeneous light field will experience a dipole gradient force resulting from the spatial gradient of the optical potentials. From the optical potentials as shown in Eq. (8), we obtain the expressions of the instantaneous dipole forces in three dressed levels, respectively

$$\mathbf{F}_1 = -\nabla U_1 = \frac{\hbar}{4}\left[\pm\frac{\Omega_1}{16\Omega_1'} \mp \frac{\frac{1}{16}\frac{\Omega_1\Delta}{\pm\Omega_1'}+\Omega_1}{\sqrt{\Delta^2+\Omega_1^2}}\right]\cdot\nabla\Omega_1, \tag{9a}$$

$$\mathbf{F}_2 = -\nabla U_2 = \frac{\hbar}{4}\left[\pm\frac{\Omega_2}{16\Omega_1'} - \mathrm{sgn}\,\frac{\frac{1}{16}\frac{\Omega_2(\Delta+\delta_{hfs})}{\pm\Omega_1'}+\Omega_2}{\sqrt{(\Delta+\delta_{hfs})^2+\Omega_2^2}}\right]\cdot\nabla\Omega_2, \tag{9b}$$

$$\mathbf{F}_3 = -\mathbf{F}_1 - \mathbf{F}_2. \tag{9c}$$

For the alkali-metal atom, $\nabla\Omega_1=\nabla\Omega_2=\sqrt{1/3(I\cdot I_{sat})}\Gamma\cdot\nabla I/2$. From Eq. (9), we calculate the dependence of the instantaneous dipole forces F_1 and F_2 on a ^{87}Rb atom on the detuning $\delta/2\pi$ as $I=10^4$ W/m^2 and $\nabla I=-10^8$ mW/cm^3, and the results are shown in Fig. 6. We can find from Fig. 6 that there is a pair of the maximum absolute values of the instantaneous dipole force at the detuning $\delta/2\pi=0$ GHz for F_1 and $\delta/2\pi=-6.835$ GHz for F_2, which comes from two nonresonant effects at $\delta/2\pi=0$ GHz and at $\delta/2\pi=-\delta_{hfs}/2\pi$, respectively. We also find from Fig. 6 that F_1 is far larger than F_2 when $\delta/2\pi>0$ GHz, which is a necessary condition for the effective IGC. From Eqs.(9) and (5a), we calculate the dependence of the radial instantaneous dipole forces F_{1r} and F_{2r} on a ^{87}Rb atom on the radius r for

$r_0=0.5$ mm, $P_1=1000$ mW, $\eta=0.28$, and $\delta/2\pi=1$ GHz, and find that the minimum radial instantaneous dipole forces F_{1r} and F_{2r} appeared at $z=(2n+1)\lambda/4$ as $r=0.25$ mm and can be reached 4.0×10^{-23} N and 5.2×10^{-24} N, which is about 28.6 and 3.7 times of the gravity force (1.4×10^{-24} N) on the ^{87}Rb atom. When the detuning is $\delta/2\pi=8$ GHz, the minimum radial instantaneous dipole forces F_{1r} and F_{2r} as $r=0.25$ mm are 5.1×10^{-24} N and 2.8×10^{-24} N. From Eqs. (9) and (5b), we also calculate the dependence of the axial instantaneous dipole forces F_{1z} and F_{2z} on a ^{87}Rb atom on the propagation distance z for $r_0=0.5$ mm, $P_1=1000$ mW, $\eta=0.28$, $r=0.25$ mm, and $\delta/2\pi=1$ GHz, and find that the axial instantaneous dipole forces F_{1z} and F_{2z} can be changed from 0 to 4.7×10^{-19} N and 6.7×10^{-20} N within the axial length of $\lambda/8$. When the detuning is $\delta/2\pi=8$ GHz, the axial maximum instantaneous dipole forces F_{1z} and F_{2z} can be reached 6.6×10^{-20} N and 3.6×10^{-20} N, which is $\sim10^4$ times of the gravity force on the ^{87}Rb atom. So when $\delta/2\pi<8$ GHz, our weak standing-wave hollow beam trap have effective axial and radial instantaneous dipole forces and make cold atoms oscillate rapidly in the trap. Typically, when $r_0=0.5$ mm, $P_1=1000$ mW, $\eta=0.28$, and $\delta/2\pi=3$ GHz, the axial mean oscillation frequency is 1.1×10^5 Hz, while the radial mean oscillation frequency is 266.4 Hz, which is a another necessary condition for the effective IGC of trapped atoms in our GOT.

C. The spontaneous emission rates

When a three-level atom moves in the weak standing-wave hollow-beam field, it will experience the spontaneous emission and its recoil heating. To obtain the spontaneous emission rates of the three-level atom in the intense laser field and perform Monte Carlo study for IGC, we substitute three dressed eigenenergies [see Eq. (7)] into Eq. (6) respectively and solve them, and then three eigenstates $|1,n\rangle$, $|2,n\rangle$, and $|3,n\rangle$ in the dressed-atomic picture can be given by

$$|i,n\rangle = A_i|g_2,n+1\rangle + B_i|g_1,n+1\rangle + C_i|e,n\rangle, \tag{10}$$

where $i=1,2,3$, and the probability amplitudes A_i, B_i, and C_i are given by

$$A_i = \frac{|a_{i2}|}{\sqrt{1+a_{i1}^2+a_{i2}^2}}, \quad B_i = \frac{|a_{i1}|}{\sqrt{1+a_{i1}^2+a_{i2}^2}},$$

$$C_i = \frac{1}{\sqrt{1+a_{i1}^2+a_{i2}^2}}, \tag{11}$$

where

$$a_{11} = \frac{-\Omega_1}{\Delta \mp \sqrt{\Delta^2+\Omega_1^2}},$$

$$a_{12} = \frac{-\Omega_2}{\Delta \mp \sqrt{\Delta^2+\Omega_1^2+2\delta_{hfs}}},$$

$$a_{21} = \frac{-\Omega_1}{\Delta-\delta_{hfs}-\mathrm{sgn}\sqrt{(\Delta+\delta_{hfs})^2+\Omega_2^2}},$$

$$a_{22} = \frac{-\Omega_2}{\Delta+\delta_{hfs}-\mathrm{sgn}\sqrt{(\Delta+\delta_{hfs})^2+\Omega_2^2}},$$

$$a_{31} = \frac{-\Omega_1}{-2(\Delta-\delta)+\delta/16-\delta_{hfs}\pm\sqrt{\Delta^2+\Omega_1^2}+\mathrm{sgn}\sqrt{(\Delta+\delta_{hfs})^2+\Omega_2^2}},$$

$$a_{32} = \frac{-\Omega_2}{-2(\Delta-\delta)+\delta/16+\delta_{hfs}\pm\sqrt{\Delta^2+\Omega_1^2}+\mathrm{sgn}\sqrt{(\Delta+\delta_{hfs})^2+\Omega_2^2}}. \tag{12}$$

In consideration of the coupling of the dressed atom with the vacuum modes, the trapped atoms will spontaneously emit fluorescent photons, and the corresponding spontaneous emission rates Γ_{ij} from $|j,n\rangle$ to $|i,n-1\rangle$ can be given by [18,19]

$$\Gamma_{ij} = B_i^2 C_j^2 \Gamma_1 + A_i^2 C_j^2 \Gamma_2, \tag{13}$$

where Γ_1 and Γ_2 are the partial spontaneous emission rates given by $\Gamma_1=q_1\Gamma$ and $\Gamma_2=q_2\Gamma$, q_1 (q_2) is the relative

branching ratio of the spontaneous emission from $\langle e|$ to $|g_1\rangle$ (or to $|g_2\rangle$).

Since the dressed state $|1,n\rangle$ contains a small mixture of the excited state [see Eq. (10)], it may spontaneously decay to a lower dressed state $|1,n-1\rangle$, $|2,n-1\rangle$, or $|3,n-1\rangle$ with the corresponding rate Γ_{i1} $(i=1,2,3)$, that is

$$\Gamma_{i1} = B_i^2 C_1^2 \Gamma_1 + A_i^2 C_1^2 \Gamma_2. \tag{14}$$

Substituting Eqs. (11) and (12) into Eq. (14), we can obtain the expressions of the spontaneous-emission rates Γ_{11}, Γ_{21}, and Γ_{31}, similarly we can also derive the expressions of Γ_{12}, Γ_{22}, Γ_{32}, Γ_{13}, Γ_{23}, and Γ_{33}. Moreover, under the approximation of small saturation parameters [20], i.e., when $\delta_j \gg \Omega_j \gg \Gamma$, Eq. (14) can be further simplified as

$$\Gamma'_{11} = \frac{\Omega_1^2}{4\delta^2}\Gamma_1 = \frac{1}{2}s_1\Gamma_1, \tag{15a}$$

$$\Gamma'_{21} = \frac{\Omega_1^2}{4\delta^2}\Gamma_2 = \frac{1}{2}s_1\Gamma_2, \tag{15b}$$

$$\Gamma'_{31} = \frac{\Omega_1^4}{16\delta^4} + \frac{\Omega_1^2\Omega_2^2}{16\delta^2(\delta+\delta_{hfs})^2}\Gamma_2 = \frac{s_1^2}{4}\Gamma_1 + \frac{s_1 s_2}{4}\Gamma_2, \tag{15c}$$

which are the same as the results in Refs. [9,10,12,16,18,20]. Similar, the approximate expressions of the spontaneous-emission rates of the atom between other dressed states are given by

$$\Gamma'_{12} = \frac{1}{2}s_2\Gamma_1, \quad \Gamma'_{22} = \frac{1}{2}s_2\Gamma_2, \quad \Gamma'_{32} = \frac{s_1 s_2}{4}\Gamma_1 + \frac{s_2^2}{4}\Gamma_2, \tag{16}$$

$$\Gamma'_{13} = \Gamma_1, \quad \Gamma'_{23} = \Gamma_2, \quad \Gamma'_{33} = \frac{s_1}{2}\Gamma_1 + \frac{s_2}{2}\Gamma_2. \tag{17}$$

In Eqs. (15)–(17), s_1 and s_2 are two saturation parameters of the three level atom and given by

$$s_1 \approx \frac{\Omega_1^2}{2\delta^2}, \quad s_2 \approx \frac{\Omega_2^2}{2(\delta+\delta_{hfs})^2}. \tag{18}$$

From Eqs. (15)–(18), we can find that the spontaneous-emission rates between dressed states satisfy the following relation: $\Gamma'_{31} \ll \Gamma'_{11}$ (Γ'_{21}), $\Gamma'_{32} \ll \Gamma'_{12}$ (Γ'_{22}), so we can neglect Γ'_{31} and Γ'_{32} in our simulations. The transition probability of $|1,n\rangle \to |3,n-1\rangle$ per reflection can be expressed as $p_{1\to3} = \int_{-\infty}^{\infty}\Gamma'_{31}dt \approx \frac{2E_\perp}{3\hbar\delta}p_{sp}$ [6], where $E_\perp = \frac{1}{2}k_B T$ is the atomic kinetic energy in the normal direction of the light field surface, and p_{sp} is the total transition probability of atom per reflection in the light field. When $T=120$ μK, $\delta/2\pi=3$ GHz, we have $p_{1\to3} \approx 2.8\times10^{-4}$ p_{sp}, meanwhile the transition probability $|2,n\rangle \to |3,n-1\rangle$ per reflection is $p_{2\to3} = \int_{-\infty}^{\infty}\Gamma'_{32}dt \approx 2.6\times10^{-5}$ p_{sp}. Therefore, we can safely neglect the transition to the state $|3,n-1\rangle$, and then Γ'_{13}, Γ'_{23}, and Γ'_{33} in Eq. (17) can also be neglected in our simulations.

IV. THE IGC AND ITS MONTE CARLO SIMULATIONS

A. The IGC of atoms in our trap

When cold atoms are released from a standard MOT placed at the center of our weak standing-wave hollow beam GOT with an initial height of H_{MOT}, they will move and bounce in our trap. In the dressed-atom picture, if an ^{87}Rb atom in the dressed state $|1,n\rangle$ spontaneously decays into the dressed state $|2,n-1\rangle$ during a reflection from the standing-wave hollow-beam light field, the reflected atom will lose part of its kinetic energy because the dressed state $|2,n-1\rangle$ is less repulsive than the dressed state $|1,n\rangle$, as shown in Eq. (8). When the atom is reflected to the nodes from antinodes of the standing-wave hollow-beam light field, the atom is pumped back to the dressed state $|1,n-1\rangle$ by the red-detuned weak repumping beam (see WRB in Fig. 2). In the repumping process, the atom reflected upwards absorbs a downward-direction photon from the RPB and reduces the kinetic energy of the atom, and results in a spontaneous geometric cooling. It is clear that two energy-loss processes mentioned above will form a closed, repeatable Sisyphus and geometric cooling cycle. In addition, the random recoils of the emitted photons during the spontaneous emission will contribute a small heating to the reflected atom.

In consideration of the IGC and the geometric cooling, and the spontaneous-emission heating as well as the recoil-induced heating from the absorption of photons, and assuming that the mean spontaneous-emission times of atom per reflection in the standing-wave hollow-beam field is β, similar to the derivation in Refs. [6,14], we can derive an equation to estimate the final equilibrium rms momentum p_{rms} of atoms in our trap

$$-\frac{1}{3}\frac{\delta_{hfs}}{\delta+\delta_{hfs}}\left(\frac{p_{\mathrm{rms}}}{\hbar k}\right)^2 - \frac{1}{q_r}\frac{p_{\mathrm{rms}}}{\hbar k} + \frac{1}{q_r^2} + \frac{\beta}{1-q_d} = 0, \tag{19}$$

where q_r (q_d) is the mean branching ratio during a transition from $|1,n\rangle$ to $|1,n-1\rangle$ after absorbing a repumping photon (a standing-wave hollow-beam photon), and β in Eq. (19) can also be obtained from Monte Carlo simulations. In particular, when $\beta=1$, the mean spontaneous-emission times of atom per reflection is one, Eq. (19) will be reduced as Eq. (5) in Ref. [14]. For an ^{87}Rb atom, $q_d=0.75$, and $q_r=0.58$. From Eq. (19), and when $\beta=0.5$, we estimate the final equilibrium rms momentum to be $p_{\mathrm{rms}} \approx 2.40\hbar k$ corresponding to a temperature of $T \approx 0.70$ μK as $\delta/2\pi=3.0$ GHz, $\eta=0.28$, and $P_1=1000$ mW, which is in good agreement with our simulated result [see Fig. 8(a)]. The corresponding Sisyphus cooling time τ_{Sisy}, or the cooling rate γ_{Sisy}, is given by [9]

$$\tau_{Sisy} = \frac{1}{\gamma_{Sisy}} \approx 4.5\frac{\delta+\delta_{hfs}}{\gamma_{sp}(1-q_d)\delta_{hfs}}, \tag{20}$$

where γ_{sp} is the spontaneous emission rate and given by $\Gamma\Omega_1^2/6\delta^2$ [6]. When $\delta/2\pi=3.0$ GHz, $\eta=0.28$, and $P_1=1000$ mW, we obtain the cooling time $\tau_{Sisy} \approx 1.0$ s for Sisyphus cooling of ^{87}Rb atoms in our trap, which is also consistent with our simulated result [see Fig. 8(a)].

B. Monte Carlo study of the IGC

We study the dynamic process of the IGC of 200 ^{87}Rb atoms in our trap by Monte Carlo simulations, and the results are shown in Fig. 7. In our semiclassical simulations, we assume that atomic motion is described as classical, and atomic internal dynamics is treated as quantum transitions between the dressed states. So the classical approximation of atomic motion in our trap should be satisfied. It is clear that when atomic temperature is closed to or below the recoil temperature of one photon, the approximation on classical motion of cold atoms in our trap cannot be valid since the wave function of atomic motion is comparable in size with the laser wavelength, and we should use quantum Monte Carlo simulations to study the dynamic process of the IGC for ultracold atoms in our trap. However, when $\delta/2\pi=3.0$ GHz, $\eta=0.28$, and $P_1=1000$ mW, the simulated lowest temperature is ~ 0.73 μK, corresponding to $\sim 2.5\hbar k$, that is, about 2.5 photon recoil momentums, which is greater than $1\hbar k$ and slightly smaller than the result ($3.2\hbar k$) of Monte Carlo simulations in Ref. [6]. So our semiclassical simulations can be approximately valid as $T \geqslant 0.7$ μK.

On the other hand, the adiabatic approximation of atomic motion in our trap should be met. In our trap, although the potential gradient is steep, the velocity of cold atoms from the MOT is small, and then the atomic motion in our trap can fulfill the adiabatic approximation condition [21]: $\hbar kv \ll |U_1 - U_2|$, where k is the wave vector, v is atomic velocity, U_1 and U_2 are two optical potentials of the hyperfine ground states of $|1,n\rangle$ and $|2,n\rangle$. For the cold ^{87}Rb atom from the MOT ($T=120$ μK), we have $\hbar kv \approx 0.0066$ mK, when $r=r0=0.5$ mm, $P_1=1000$ mW, $\eta=0.28$, and $\delta/2\pi=3$ GHz, $|U_1 - U_2|$ is increased from 0.43 mK at the node to 4.3 mK at the antinode, which are far larger than $\hbar kv \approx 0.0066$ mK. So the motion of cold atoms in our weak standing-wave trap is adiabatic, similar to the case of Sisyphus cooling of a three-level atom in a bichromatic standing-wave field [4], and also similar to the case of blue detuned, dark optical lattice with a similar intensity gradient where the adiabatic cooling can even be realized [22].

In our simulations, the initial positions and velocities of cold atoms in the ^{87}Rb MOT are described by the Gaussian distribution, and the rms momentum of cold atoms in the MOT is $30\hbar k$ ($T \approx 120$ μK), and the diameter of the MOT is $D_{\mathrm{MOT}}=0.5$ mm. The power of the input hollow beam is $P_1=1000$ mW and its beam radius is $r_0=0.5$ mm. The detuning of the blue-detuned plug beam is 3.0 GHz, and its power and beam radius are 1000 mW and 0.5 mm, respectively. When $r=0.5$ mm, the corresponding optical potential for cold ^{87}Rb atoms at the upper hyperfine ground state is $U_2 \approx 4.28$ mK, which is far higher than the initial temperature of cold ^{87}Rb atoms (~ 120 μK). The corresponding optical dipole force on an ^{87}Rb atom at the position $r=0.5$ mm is 1.17×10^{22} N, which corresponds to about 100 times of the gravity force on the atom. This shows that the blue-detuned Gaussian plug beam can be used to efficiently trap and reflect cold atoms from the MOT with a height smaller than 20 mm.

Figure 7(a) shows the time evolution of the average height of cold atoms for two MOT height of $H_{\mathrm{MOT}}=3$ mm and 5 mm, $\eta=0.28$ and $\delta/2\pi=3.0$ GHz. It is clear from Fig. 7(a) that with the increasing of the laser cooling time, the average height of cold atoms in our trap is decreased with an oscillation and finally reaches an equilibrium height of about 0.8 mm above $z=0$ due to the effective IGC. Figure 7(b)

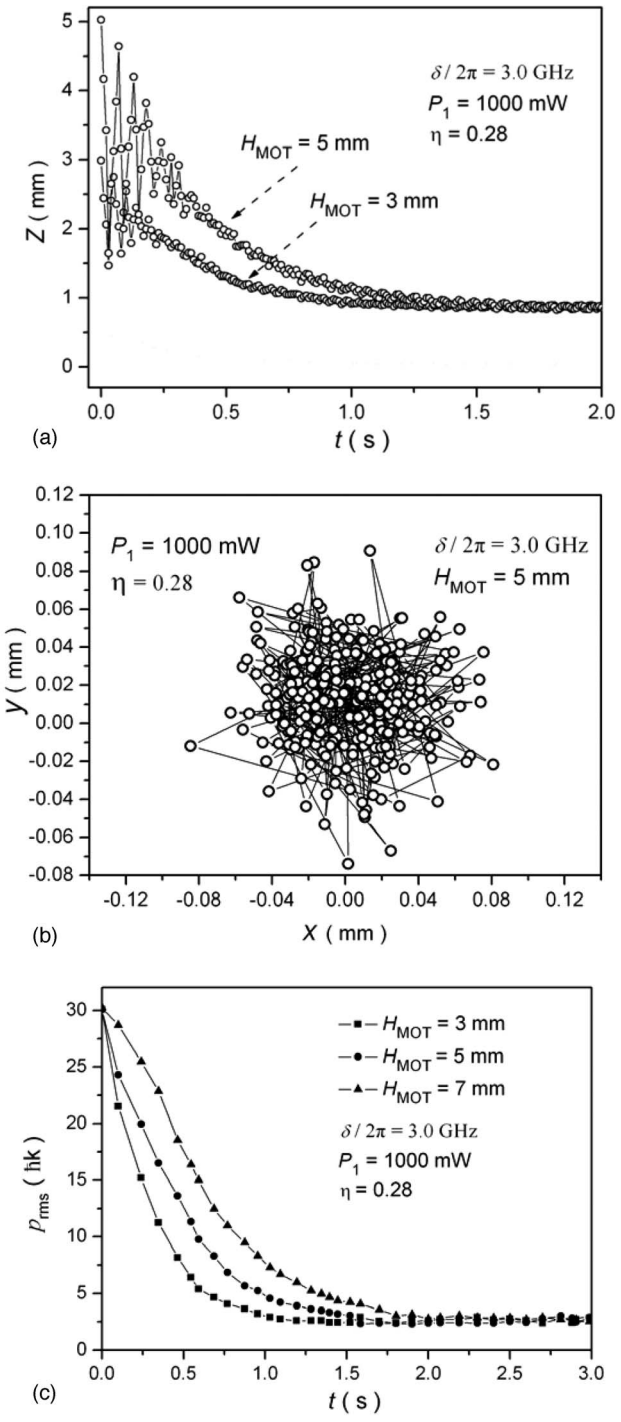

FIG. 7. (a) The evolution of atomic average height with the laser cooling time for the different heights of the MOT, $P_1=1000$ mW, $\eta=0.28$, and $\delta/2\pi=3.0$ GHz; (b) Atomic average trajectory in the x-y plane for $P_1=1000$ mW, $\eta=0.28$, $\delta/2\pi=3.0$ GHz, and $H_{\mathrm{MOT}}=5$ mm; (c) The evolution of the final rms momentum p_{rms} of atoms with the laser cooling time for the different heights of the MOT, $P_1=1000$ mW, $\eta=0.28$, and $\delta/2\pi=3.0$ GHz.

shows the average position and its trajectory of cold atoms in our trap in the x-y plane. From Fig. 7(b), we find that cold atoms from the MOT is confined in a radius of 0.08 mm in the x-y plane, and the radius of the mean atomic trajectory is reduced with increasing of the cooling time due to the IGC.

The time evolution of the final rms momentum of atoms in our trap for different heights of the MOT (H_{MOT}=3 mm, 5 mm, and 7 mm) is plotted in Fig. 7(c) for η=0.28 and $\delta/2\pi$=3.0 GHz. We can see from Fig. 7(c) that the final rms momentum of atoms ($2.45\hbar k$) is not related to the height of the MOT and the corresponding final equilibrium temperature is about 0.73 μK, which is in good agreement with theoretically predicted result ($T\approx 0.70$ μK), but the cooling time will be increased with the increase of the MOT's height, and the cooling time are about 1.4 s, 1.7 s, and 2.1 s, respectively for H_{MOT}=3 mm, 5 mm, and 7 mm.

C. Dependence of the IGC on the laser detuning $\delta/2\pi$

We study the dependence of the IGC of 200 ^{87}Rb atoms in our trap on the laser detuning $\delta/2\pi$ for H_{MOT}=3 mm, η =0.28, and P_1=1000 mW by Monte Carlo simulations, and the results are shown in Fig. 8. In which, Fig. 8(a) shows the time evolution of the final rms momentum of an atomic ensemble in our trap for the different laser detuning ($\delta/2\pi$ =1.0 GHz, 2.0 GHz, and 3.0 GHz). From Fig. 8(a), we find that the final rms momentum of cold atoms in our GOT will be reached $4.79\hbar k$ ($T\approx 2.77$ μK), $3.26\hbar k$ ($T\approx 1.28$ μK) and $2.45\hbar k$ ($T\approx 0.73$ μK), respectively for $\delta/2\pi$=1.0 GHz, 2.0 GHz, and 3.0 GHz, and the corresponding cooling times are not nearly dependent on the laser detuning $\delta/2\pi$. This shows that the final rms momentum of cold atoms in our GOT will strongly depend on the detuning $\delta/2\pi$.

Figure 8(b) presents the dependence of the final equilibrium temperature of cold atoms on the laser detuning as H_{MOT}=3 mm and η=0.28. We can see from Fig. 8(b) that: (1) the final equilibrium temperature of the trapped atoms will be increased drastically from ~2.5 μK to ~25 μK (even to higher temperature) with the reduction of the laser detuning $\delta/2\pi$ from 1 GHz to 0.5 GHz when the detuning is very small (such as $\delta/2\pi<1.0$ GHz). This is because when the detuning is very small, the spontaneous-emission heating of atoms in our GOT will be greater than the IGC, and the heating rate will be fast increased with the reduction of the detuning, which will result in a drastic increasing of the final equilibrium temperature of cold atoms in our trap. (2) When the laser detuning is larger (such as $\delta/2\pi>5.0$ GHz), the final equilibrium temperature of the cold atoms in our GOT will be increased slowly from ~2.5 μK to ~12.5 μK with the increasing of the detuning from 5.0 GHz to 9.0 GHz. This is because with increasing of the laser detuning, the energy loss per cooling cycle (which is determined by U_1-U_2) will be reduced, that is, the IGC will be decreased. At the same time, the corresponding spontaneous-emission heating will be also reduced, but the reduction of the cooling rate is faster than decreasing of the heating one, and then the final equilibrium temperature will be also increased with the increasing of the detuning. (3) There is an efficient laser cooling range (1.0 GHz$\leqslant\delta/2\pi\leqslant$5.0 GHz) and a minimum final

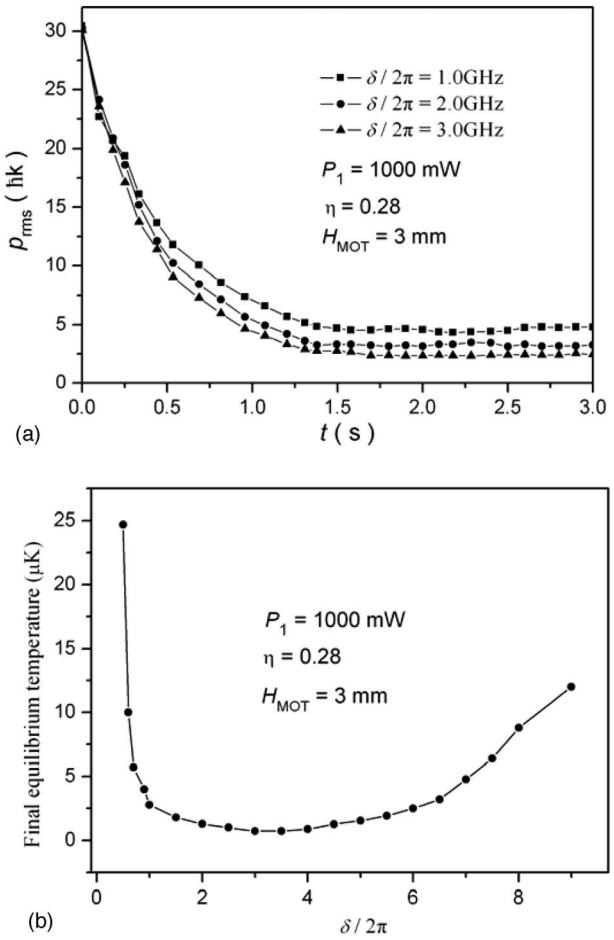

FIG. 8. (a) The evolution of the final rms momentum p_{rms} of atoms with the laser cooling time from Monte Carlo simulations for the different detuning, P_1=1000 mW, η=0.28, and H_{MOT}=3 mm; (b) The final equilibrium temperature of an ensemble of atoms versus the detuning for P_1=1000 mW, η=0.28, and H_{MOT}=3 mm.

equilibrium temperature of ~0.73 μK at $\delta/2\pi$=3.0 GHz, which is consistent with the theoretically predicted result (0.70 μK) estimated by Eq. (19) as the same detuning and parameters are used. It is clear from the above results and analysis that the final equilibrium temperature of an ensemble of atoms will be determined by a difference between the IGC and the spontaneous-emission heating and their rate difference, which will strongly depend on the laser detuning $\delta/2\pi$.

D. Dependence of the IGC on the standing-wave parameter η

We also study the dependence of the IGC of ^{87}Rb atoms in our GOT on the standing-wave parameter η, and the results are shown in Fig. 9. In which, Fig. 9(a) shows the time evolution of the final rms momentum of cold atoms for H_{MOT}=3 mm, $\delta/2\pi$=3.0 GHz, and η=0.28, 0.2, 0.1, and 0.01. We can find from Fig. 9(a) that the final rms momentum of atoms in our trap can be reached $2.45\hbar k$, $4.16\hbar k$, $5.77\hbar k$, and $10.85\hbar k$ when η=0.28, 0.2, 0.1, and 0.01 respectively, and the final rms momentum of atoms as well as

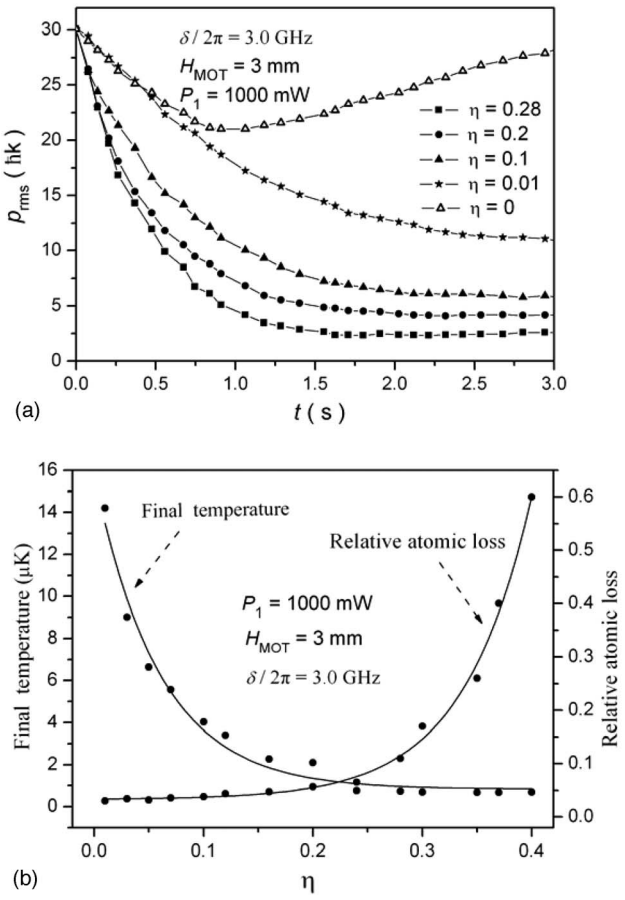

FIG. 9. (a) The evolution of the final rms momentum p_{rms} of atoms with the laser cooling time for the different η, P_1 =1000 mW, $\delta/2\pi$=3.0 GHz, and H_{MOT}=3 mm; (b) The final equilibrium temperature of an ensemble of atoms and the relative atomic loss versus η for P_1=1000 mW, $\delta/2\pi$=3.0 GHz, and H_{MOT}=3 mm.

the cooling time will be reduced with the increasing of the standing-wave parameter η. This is because the intensity gradient of our weak standing-wave hollow beam field will be increased with the increasing of the parameter η. The corresponding final equilibrium temperature versus the standing-wave parameter η is shown in Fig. 9(b). Although the final equilibrium temperature will be decreased with the increasing of the parameter η, and the minimum optical potential U_2 at the nodes will be decreased, as shown in Fig. 5(b), which will reduce the trapping ability and result in more cold atoms to be lost from our trap, and the dependence of relative atomic loss on the parameter η is also shown in Fig. 9(b). Furthermore, we find from Fig. 9(b) that when the parameter η is larger than 0.25, the final equilibrium temperature will be decreased much slowly, but the relative atomic loss in our GOT will be increased fast. So there is an optimal choosing for the standing-wave parameter η, and our study shows that the choosing range of the parameter η should be smaller than 0.28, and the corresponding atomic loss is smaller than 10%

Moreover, we also study the IGC of ^{87}Rb atoms in a single traveling-wave hollow-beam trap as η=0, and the simulated result is shown in Fig. 9(a). We find from Fig. 9(a) that the rms momentum of cold atoms will be decreased from 30$\hbar k$ to 21.01$\hbar k$ (53.3 μK) with the increasing of the time from 0 s to 0.9 s at $\delta/2\pi$=3 GHz, and then increased to 28.34$\hbar k$ at 3 s, and this result shows that the IGC effect of atoms in a single traveling-wave hollow beam trap is far lower than that in a weak standing-wave hollow beam one, and the final rms momentum of cold atoms will be equal to even larger than the initial rms momentum of cold atoms from the MOT. This is because the axial intensity gradient of the single traveling-wave hollow beam is zero, and the IGC of atoms will only result in its radial intensity gradient.

V. CONCLUSIONS

We have proposed a unique GOT scheme to trap and cool atoms simultaneously by using a weak standing-wave hollow beam field and derived more exact and general quasianalytic expressions on the optical potentials, instantaneous dipole forces and spontaneous emission rates for a three-level dressed-atom system. We have also studied the dynamic processes of the IGC of atoms in our GOT by Monte Carlo simulations, and investigated the dependence of the IGC on both the laser detuning $\delta/2\pi$ and the standing-wave parameter η. Our study found that (1) that the derived general expressions on the optical potentials, instantaneous dipole forces and spontaneous emission rates are valid for any laser detuning (including a resonant frequency position of $\delta/2\pi$ =0) and the resulting maximum relative error is only ~3% as $I \leqslant 2.5\times 10^6$ W/m^2, which has been the most exact solutions for a three-level atomic system so far, so they could be safely used to study the interaction between a three-level atom and a strong laser field with an arbitrary detuning so long as $I \leqslant 2.5\times 10^6$ W/m^2.

(2) The IGC of atoms in our GOT is not only related to the laser detuning $\delta/2\pi$, but also strongly depends on the standing-wave parameter η, and there is an efficient and wide laser cooling range (such as 1.0 GHz$\leqslant \delta/2\pi \leqslant$5.0 GHz) and an optimal detuning (such as $\delta/2\pi$ =3.0 GHz) and standing-wave parameter η (e.g., η=0.28), where an optimized final equilibrium temperature can be obtained, which can provide some reliable theoretical basis for further experimental study of the IGC of atoms in the weak standing-wave hollow-beam GOT.

(3) The IGC of atoms in our GOT is very efficient, and can be used to directly cool alkali-metal atoms from a MOT's temperature to one with a few photon recoils. For example, an ^{87}Rb atomic sample in our trap can be directly cooled to an equilibrium temperature of ~0.73 μK (~2.45$\hbar k$) from ~120 μK by our IGC. To our knowledge, this to date is the best cooling result (~0.73 μK) in two kinds of sub-Doppler cooling mechanisms (i.e., the PGC and IGC).

In addition, there is also the IGC of atoms in a traveling-wave hollow beam trap since there is a weak radial intensity gradient inside a single hollow beam, but its Sisyphus cooling effect is far lower than one in our weak standing-wave hollow beam trap.

Compared with other optical dipole traps or GOTs, our proposed GOT has some unusual and unique advantages as

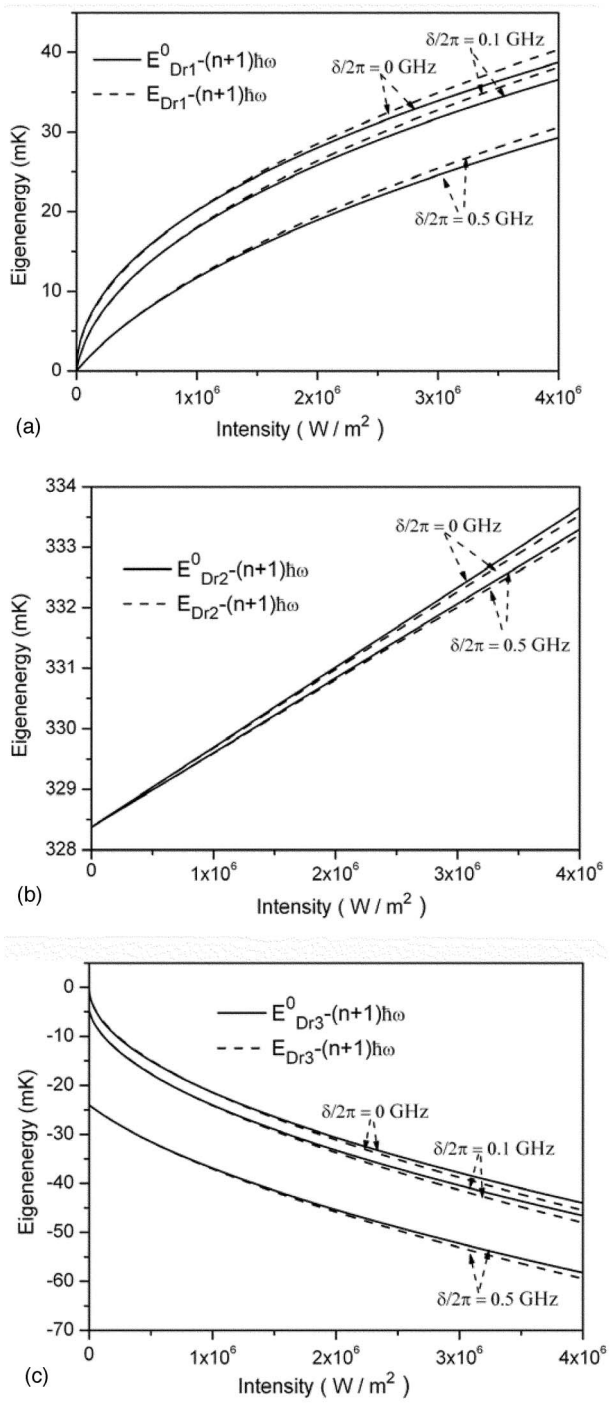

FIG. 10. (a) Dependences of $E^0_{Dr1}-(n+1)\hbar\omega_L$ and $E_{Dr1}-(n+1)\hbar\omega_L$ on the laser intensity I for $\delta/2\pi=0$ GHz, 0.1 GHz, and 0.5 GHz; (b) Dependence of $E^0_{Dr2}-(n+1)\hbar\omega_L$ and $E_{Dr2}-(n+1)\hbar\omega_L$ on the intensity I for $\delta/2\pi=0$ GHz and 0.5 GHz; (c) Dependence of $E^0_{Dr3}-(n+1)\hbar\omega_L$ and $E_{Dr3}-(n+1)\hbar\omega_L$ on the intensity I for $\delta/2\pi=0$ GHz, 0.1 GHz, and 0.5 GHz.

follows: (1) It cannot only be used to trap cold atoms (or cold molecules), but also to efficiently cool neutral atoms to about 0.73 μK from ~120 μK (the MOT temperature) by using the intensity-gradient induced Sisyphus cooling of our GOT oneself; (2) It is more convenient and flexible to manipulate and control the motion of cold atoms in our trap, even to control the cooling temperature and lose rate of atoms in the trap by changing the standing-wave parameter η; (3) It is desirable and promising to realize the optical-potential evaporative cooling of atoms in our GOT by reducing the intensities at the nodes of our standing-wave hollow beam, and so on. Therefore, our GOT scheme cannot only be used to study cold collisions between two atomic (molecular) samples or between atomic and molecular samples, but also to realize optical-potential evaporative cooling of an atomic (molecular) gas [23] and sympathetic cooling between ultracold atoms and cold molecules, even to prepare all-optical two-dimensional (2D) BEC [24,25] or all-optical 2D quantum Fermionic gases [26] by lowering the trapping laser power [25] or by increasing the standing-wave parameter η so as to let hotter atoms escape from a series of nodes, and to generate all-optical quantum molecular gases [27–29] or realize a toroidal optical dipole trap in 2D BEC [30] as well as to study quantum atom statistics [31], and so on.

ACKNOWLEDGMENTS

This work was supported by the National Natural Science Foundation of China under Grant Nos. 10174050, 10374029, and 10434060, Shanghai Priority Academic Discipline and the 211 Foundation of the Educational Ministry of China.

APPENDIX A: DERIVATION OF EXACT SOLUTIONS OF EQ. (6)

To obtain the eigenenergies in the dressed-atom picture, from Eq. (6), we should solve the following equation:

$$\begin{vmatrix} (n+1)\omega_L+\delta_{hfs}-E_{Dr} & 0 & \frac{\Omega_2}{2} \\ 0 & (n+1)\omega_L-E_{Dr} & \frac{\Omega_1}{2} \\ \frac{\Omega_2}{2} & \frac{\Omega_1}{2} & n\omega_L+\omega_0-E_{Dr} \end{vmatrix} = 0. \tag{A1}$$

It is clear that the Eq. (A1) can be simplified as a standard cubic equation with one unknown variable, and its general solutions are given by

$$E^0_{Dr1}=(n+1)\hbar\omega_L-\frac{\delta-\delta_{hfs}}{3}+\sqrt[3]{-q+i\sqrt{-(q^2+p^3)}}+\sqrt[3]{-q-i\sqrt{-(q^2+p^3)}}, \tag{A2a}$$

$$E^0_{Dr2}=(n+1)\hbar\omega_L-\frac{\delta-\delta_{hfs}}{3}+\sqrt[3]{-q+i\sqrt{-(q^2+p^3)}}\frac{-1+i\sqrt{3}}{2}+\sqrt[3]{-q-i\sqrt{-(q^2+p^3)}}\frac{-1-i\sqrt{3}}{2}, \tag{A2b}$$

$$E^0_{Dr3} = (n+1)\hbar\omega_L - \frac{\delta - \delta_{hfs}}{3} + \sqrt[3]{-q + i\sqrt{-(q^2+p^3)}}\frac{-1-i\sqrt{3}}{2} + \sqrt[3]{-q - i\sqrt{-(q^2+p^3)}}\frac{-1+i\sqrt{3}}{2}, \quad \text{(A2c)}$$

where

$$p = -\left(\frac{\delta - \delta_{hfs}}{3}\right)^2 - \frac{\Omega_1^2 + \Omega_2^2 + 4\delta\delta_{hfs}}{3\times 4}, \quad \text{(A3a)}$$

$$q = \left(\frac{\delta - \delta_{hfs}}{3}\right)^3 + (\delta - \delta_{hfs})\frac{\Omega_1^2 + \Omega_2^2 + 4\delta\delta_{hfs}}{3\times 8} + \frac{\Omega_1^2\delta_{hfs}}{8}. \quad \text{(A3b)}$$

APPENDIX B: COMPARISON BETWEEN OUR ANALYTIC SOLUTIONS AND EXACT ONES

Taking ^{87}Rb atoms as an example, we compared our analytic solutions E_{Dri} in Eq. (7) with the exact solutions E^0_{Dri} in Eq. (A2), here $i=1,2,3$. For a ^{87}Rb atom, $\delta_{hfs}/2\pi = 6.835$ GHz, $I_{sat}=16$ W/m^2 m and $\Gamma/2\pi=6.0$ MHz. From Eqs. (7) and (A2), we obtain the dependence of $E^0_{Dri}-(n+1)\hbar\omega_L$ and $E_{Dri}-(n+1)\hbar\omega_L$ on the laser intensity I for different detuning, and the results are shown in Fig. 10. We can find from Fig. 10 that the maximum relative errors between $E_{Dr1}-(n+1)\hbar\omega_L$ and $E^0_{Dr1}-(n+1)\hbar\omega_L$ are less than 2.4%, 2.6%, 3.0% as $I\leqslant 2.5\times 10^6$ W/m^2 and $\delta/2\pi=0$ GHz 0.1 GHz, 0.5 GHz, respectively [see Fig. 10(a)], while the maximum relative errors between $E_{Dr2}-(n+1)\hbar\omega_L$ and $E^0_{Dr2}-(n+1)\hbar\omega_L$ are about 0.016% and 0.012% as $I\leqslant 2.5\times 10^6$ W/m^2, $\delta/2\pi=0$ GHz and 0.5 GHz, respectively [see Fig. 10(b)]. Similarly, the maximum relative errors between $E_{Dr3}-(n+1)\hbar\omega_L$ and $E^0_{Dr3}-(n+1)\hbar\omega_L$ are less than 2.0%, 1.9%, and 1.3% as $I\leqslant 2.5\times 10^6$ W/m^2, $\delta/2\pi=0$ GHz 0.1 GHz, and 0.5 GHz, respectively [see Fig. 10(c)]. We also obtain the dependence of $E^0_{Dr1}-(n+1)\hbar\omega_L$ and $E^0_{Dr2}-(n+1)\hbar\omega_L$ on the detuning $\delta/2\pi$ as $I=2.5\times 10^6$ W/m^2, and the results are shown in Fig. 11. We analyze the dependence of the relative errors between $E_{Dri}-(n+1)\hbar\omega_L$ and $E^0_{Dri}-(n+1)\hbar\omega_L$ on the detuning, and find that the maximum relative error is about 3.0% as $I=2.5\times 10^6$ W/m^2 for arbitrary detuning $\delta/2\pi$. This shows that Eq. (7) can be used to more exactly calculate the eigenenergies E_{Dri} of dressed eigenstates $|i,n\rangle$, and the resulting maximum relative error is only $\sim$3% for arbitrary detuning $\delta/2\pi$ as $I<2.5\times 10^6$ W/m^2. It can be seen from the above analysis that some coefficients in Eq. (7) are somewhat surprising, but Eq. (7) can be indeed regarded as a general and more exact solution of Eq. (6) and safely used to calculate the eigenenergies E_{Dri} and their optical potentials [in fact, $E_{Dr1}-(n+1)\hbar\omega_L$ is the optical potential of the dressed-eigenstates $|1,n\rangle$] and eigenstates and so on for arbitrary detuning and $I\leqslant 2.5\times 10^6$ W/m^2.

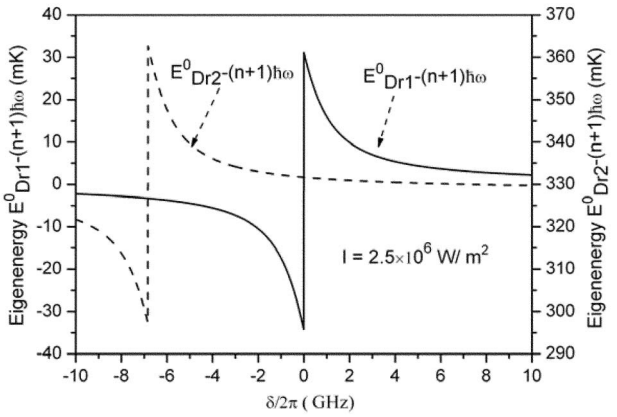

FIG. 11. Dependences of $E^0_{Dr1}-(n+1)\hbar\omega_L$ and $E^0_{Dr2}-(n+1)\hbar\omega_L$ on the laser detuning $\delta/2\pi$ for $I=2.5\times 10^6$ W/m^2.

[1] J. Dalibard and C. Cohen-Tannoudji, J. Opt. Soc. Am. B **6**, 2023 (1989).
[2] J. Yin, W. Gao, and Y. Zhu, Prog. Opt. **45**, 119 (2003).
[3] D. V. Kosachiov, Yu. V. Rozhdestvensky, and G. Nienhuis, J. Opt. Soc. Am. B **14**, 535 (1997).
[4] R. Gupta, C. Xie, S. Padua, H. Batelaan, and H. Metcalf, Phys. Rev. Lett. **71**, 3087 (1993).
[5] Yu. B. Ovchinnikov, J. Soding, and R. Grimm, JETP Lett. **61**, 10 (1995).
[6] J. Soding, R. Grimm, and Yu. B. Ovchinnikov, Opt. Commun. **119**, 652 (1995).
[7] Yu. B. Ovchinnikov, L. Manek, and R. Grimm, Phys. Rev. Lett. **79**, 2225 (1997).
[8] J. Yin and Yifu Zhu, J. Opt. Soc. Am. B **15**, 2235 (1998).
[9] J. Yin, Y. Zhu, and Y. Wang, Phys. Rev. A **57**, 1957 (1998).
[10] J. Yin, Y. Zhu, W. Jhe, and Y. Wang, Phys. Rev. A **58**, 509 (1998).
[11] O. Morsch and D. R. Meacher, Opt. Commun. **148**, 49 (1998).
[12] J. Yin and Y. Zhu, Opt. Commun. **152**, 421 (1998).
[13] Yu. B. Ovchinnikov, L. Manek, A. I. Sidorov, G. Wasik, and R. Grimm, Europhys. Lett. **43**, 510 (1998).
[14] J. Yin, W. Gao, Y. Zhu, and Y. Wang, Phys. Lett. A **288**, 9 (2001).
[15] V. I. Balykin, D. V. Laryushin, M. V. Subbotin, and V. S. Letokhov, JETP Lett. **63**, 802 (1996).
[16] J. Yin, Y. Zhu, and Y. Wang, Phys. Lett. A **248**, 309 (1998).
[17] Z. Wang, M. Dai, and J. Yin, Opt. Express **13**, 8406 (2005).
[18] X. Xu, Y. Wang, and W. Jhe, J. Opt. Soc. Am. B **17**, 1039 (2000).
[19] J. Dalibard and C. Cohen-Tannoudji, J. Opt. Soc. Am. B **2**, 1707 (1985).
[20] H. Nha and W. Jhe, Phys. Rev. A **56**, 729 (1997).
[21] G. Grynberg and C. Robilliard, Phys. Rep. **355**, 335 (2001).
[22] V. Elman and A. Hemmerich, Phys. Rev. A **72**, 043410 (2005).
[23] M. Hammes, D. Rychtari, B. Engeser, H. C. Nagerl, and R. Grimm, Phys. Rev. Lett. **90**, 173001 (2003).

[24] D. Rychtarik, B. Engeser, H. C. Nagerl, and R. Grimm, Phys. Rev. Lett. **92**, 173003 (2004).
[25] J. Yin, Phys. Rep. **430**, 1 (2006).
[26] J. P. Martikainen and P. Torma, Phys. Rev. Lett. **95**, 170407 (2005).
[27] J. Herbig, T. Krasmer, M. Mark, T. Weber, C. Chin, H. C. Nagerl, and R. Grimm, Science **301**, 1510 (2003).
[28] J. Cubizolles, T. Bourdel, S. J. J. M. F. Kokkelmans, G. V. Shlyapnikov, and C. Salomon, Phys. Rev. Lett. **91**, 240401 (2003).
[29] H. Moritz, T. Stoferle, K. Gunter, M. Kohl, and T. Esslinger, Phys. Rev. Lett. **94**, 210401 (2005).
[30] E. M. Wright, J. Arlt, and K. Dholakia, Phys. Rev. A **63**, 013608 (2000).
[31] T. P. Meyrath, F. Schreck, J. L. Hanssen, C. S. Chuu, and M. G. Raizen, Phys. Rev. A **71**, 041604 (2005).